Design of High-Power Polyphase PCB Coil Systems for Wireless Power Transfer

Donovin D. Lewis[1], Lucas Gastineau[1], Omer Onar[2], Malcolm McCulloch[3]
John F. Eastham[4], and Dan M. Ionel[1]
[1]SPARK Laboratory, Stanley and Karen Pigman College of Engineering, University of Kentucky, Lexington, KY, USA
[2]Vehicle Power Electronics Research Group, Oak Ridge National Laboratory, Knoxville, TN, USA
[3]EPG, Department of Engineering Science, University of Oxford, Parks Road, Oxford, OX1 3PJ, UK
[4]Department of Electronic and Electrical Engineering, University of Bath, Claverton Down, Bath, BA2 7AY, UK
donovin.lewis@uky.edu, lucas.gastineau@uky.edu, onaroc@ornl.gov,
malcolm.mcculloch@eng.ox.ac.uk, jfeastham@aol.com, dan.ionel@ieee.org

***Abstract*—Printed circuit board (PCB) coils have been proposed prior for implementation as inductive wireless charging coils to minimize size and cost. Utilization of PCBs can allow for a reduced cost, improved manufacturability, and a wide range of geometric customization options. To circumvent material limitations on insulation and thermal performance, parallel paths can be implemented to divide the current per path accordingly. Within this paper, an unconventional high-power PCB coil is designed employing all possible techniques for wiring with axial and radial parallel paths with equivalent transposition to minimize circulating currents. Design studies are simulated in 3D finite element analysis (FEA) to evaluate imbalance between phases with and without transposition. Two experimental prototype coils were fabricated with measurements for self-inductance and mutual inductance between phases. These measurements were validated to be sufficiently consistent with FEA results. Additionally, a method is proposed for a two-step optimization of coupling coefficient and coil losses.**

***Index Terms*—Wireless power transfer, planar coil, transposition, printed circuit board, wireless charging.**

I. Introduction

This paper aims to address if rated power can be increased in polyphase printed circuit board (PCB) coils for wireless power transfer (WPT) without significant imbalances by combining parallel paths and conductor transposition. Wireless charging of electric vehicles has been of recent interest with potential benefits including improved user convenience, safety of operation, and battery size reduction. Typical requirements for this application include high transmission efficiency across a large airgap and maximum volumetric and gravimetric power density on the vehicle-side [1].

High-power wireless charging coils typically use Litz wire due to the capability for many small parallel strands with equal inductance and resistance to share current equally and mitigate eddy currents at high-frequency [2]. Transposition of Litz wire strands also significantly mitigates circulating currents by reducing imbalances between parallel paths. While Litz wire offers very high-power capability, they have limited availability, constraints on geometry configurations, and intensive assembly requirements resulting in a relatively high cost. Alternative manufacturing with PCBs employs routed copper conductor traces on interconnected planes for significantly reduced volume and cost, improved repeatability, and high configurability.

In recent years, the application of PCBs has been expanded to windings for electromagnetic circuits including electric machines, transformers, and wireless chargers [3]. Ideal implementations of PCB coils for wireless electric vehicle charging may be for a large traditional primary coil embedded in the ground and a very thin, lightweight, and cost-effective PCB on the secondary-side such as those proposed prior in [4] and [5]. The restricted fill factor greatly impacts performance of PCB electromagnetics compared to Litz wire as discussed in [6] with significantly reduced capability to scale rated power. As a result, the majority of previously proposed PCB coils for WPT have rated powers at 3.3kW or lower. Multiple methods have been proposed to increase overall cross-sectional copper area with parallel paths including, for example, parallel layer connections from [7] and planar slits as in [8].

The capability to add parallel connections while maintaining interphase or interlayer balance varies depending on coil topology. Polyphase WPT coils, like those discussed in [9], have been developed recently for improved power density and specific power compared to single phase alternatives at a similar size due to increased field utilization. Differences in conductor proximity to the ferrite core can significantly vary inductance, causing differing induced voltage and large circulating currents as explored in [10]. The configurability and interplanar connections of PCBs allow for coil transposition to equalize field magnetic field distribution across conductors. Examples of multi-layer conductor design in literature include layer transition per pole [7], Litz-structure braiding or interleaved parallel planar segments [11], [12], and interturn conductor radii variation [13].

This study develops a new method of conductor transposition to enable high-power (11kW) 85kHz PCB WPT using parallel connections in a three-phase coil configuration. Electromagnetic finite element analysis in ANSYS Maxwell [14] and experimental measurements are used to evaluate the effectiveness of a transposition for three-phase coils to allow for increased parallel paths without large interphase and interlayer imbalances. A 3-phase, 3-layer coil topology, depicted in

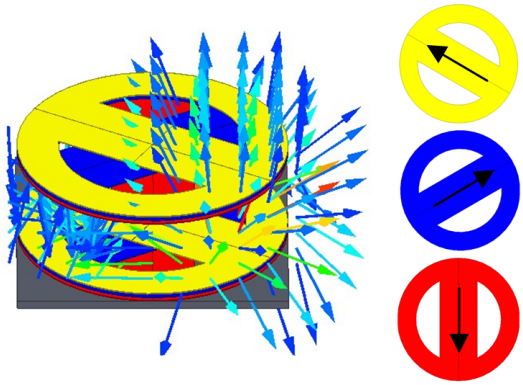

Fig. 1. Electromagnetic finite element model of the three-phase two-pole rotating-field wireless power transfer coil studied in a PCB form factor with the secondary-side ferrite omitted for clarity. Expected imbalance between phases and layers is mitigated through additional measures.

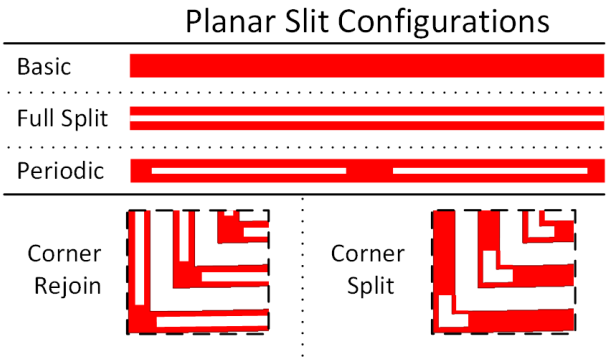

Fig. 2. Slit types to connect planar turns for additional current capacity. Size and occurrence are determined by the trade-off between DC and AC losses.

Fig. 1 and previously explored in [15], was selected due to its high specific power with the maximum active coil area for a bipolar coil in a rotating field configuration. Results from two prototype coils, one with transposition, are described and have satisfactory agreement with 3D FE simulations, indicating the capability for improved performance with parallel PCB layers.

II. Rotating Three-Phase Two-Pole Coil Coupler

The coil topology for analysis, optimization, and experimental development is a rotating-field 3 phase, 3-layer two pole coil which benefits from the highest utilization of active area, allowing for many turns and an intense and well concentrated field. The coil, shown in Fig. 1, uses phase-shifted excitation and spatially shifted coils to create the rotating fields for constant power transfer. While the topology was presented in [16] as one of the possible polyphase configurations with high specific power and field utilization, there are certain difficulties to realize this topology with Litz wire due to bend radii restrictions. As a result, it has not been implemented before. The rotating magnetic field excitation has improved space-time field utilization with improved power density compared to single-phase coils.

Power within the selected topology can be calculated with the following equation from [16]:

$$P = \frac{9}{2}\omega M_{ps} I_p I_s \tag{1}$$

where M_{ps} is the mutual inductance between the two coils, I_p the current in the primary, and I_s the current in the secondary. An inductance limit is typically defined to restrict the size of accompanying compensation components. Due to the limitations in current capability in existing PCB designs, a trade-off exists between maximal inductance to minimize current needed for rated power and the increased size and cost of accompanying compensation. Compared to other multi-pole geometries, the two-pole configuration for multi-phase rotating field couplers allows for the largest area for turns or parallel planar paths per layer as it is fully pitched.

Rated power and mutual inductance per turn naturally increases with larger coil outer diameter (OD), reducing the necessary current for the same rated power. As a result, the coil OD should be as wide as possible for the system, allowing for larger airgaps and less turns for the rated mutual inductance. Increases to coil OD may also allow for more parallel planar connections, like the examples in Fig. 2, to increase current capability. This study assumes a 100mm OD to isolate factors which can be changed outside of the restricted horizontal size.

III. Design Techniques to Increase Power in PCB-based Electromagnetic Devices

Limits on minimum spacing between conductors with standard FR4 laminate, as defined in IPC-2221 [17], a standard on printed circuit board manufacturing, significantly restricts fill factor. allowing for less current for similar thermal performance as Litz wire. Minimization of losses requires a trade-off between reduced DC resistance and eddy current losses as high excitation frequency creates eddy currents which scale with conductor size compared to the skin depth:

$$\delta = 1/\sqrt{\pi f \mu \sigma} \tag{2}$$

where σ is the material conductivity, f the operating frequency, and μ is material permeability. A high frequency of 85kHz was selected based on the SAEJ2954 standard [18] for electric vehicle charging. A sufficient reduction of eddy current losses is assumed by using dimensions equal to the skin depth, restricting copper conductor width and height accordingly.

Resistance in the copper conductors can be estimated with: $R = N\frac{pL}{A}$ where N is the number of turns, p the resistivity, L the average length of the conductor per turn, and A the cross-sectional area of the conductor. If the resistive losses are unacceptable at the current necessary for rated power, additional parallel paths may be added radially or axially to split the current. Parallel planar connections, with examples shown in Fig. 2, can be implemented to reduce the resistive losses but require slits to mitigate eddy current losses, the optimal configuration of which requires further exploration. Series connections between layers, like those used in [19], have naturally balanced inductance and can increase the number of possible planar parallel paths.

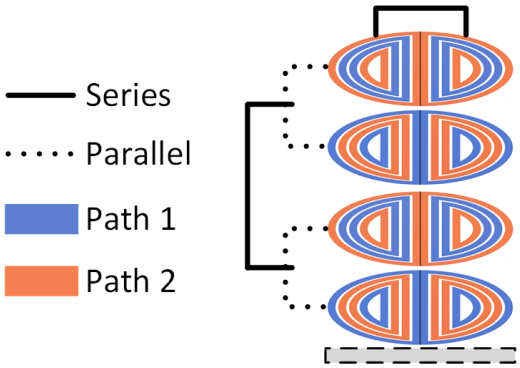

Fig. 3. An example layer-to-layer and turn transposition for a single-phase PCB WPT coil with four layers, and four turns per grouped turn. This configuration allows for one planar parallel path and one axial parallel layer for additional current capacity.

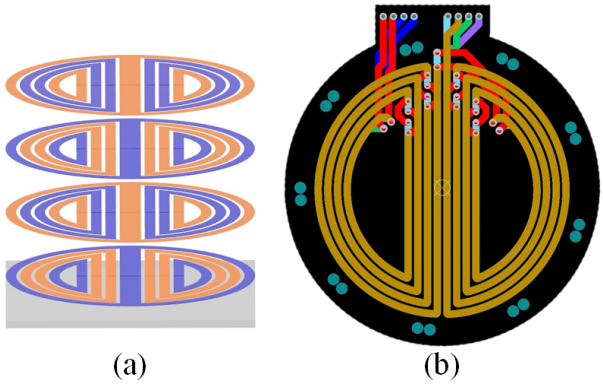

Fig. 4. Assembly view of the 3D FEA model created to evaluate the effectiveness of the proposed transposition (a) and a PCB design of the transposition without fine turns (b).

Parallel axial connections between layers increase current capacity but can result in different induced voltage from varying proximity to the ferrite core. Differences in induced voltages between phases can cause large currents due to low resistance. Imbalances in self-inductance between phases increase costs by requiring three different capacitor sizes for compensation rather than one. For the studied topology, the straightforward sequential layer implementation of phases also results in significant imbalances between phases, requiring transposition for mitigation.

A single-phase example of the transposition with the highest likelihood of minimum phase to phase imbalance and parallel connections is shown in Fig. 3. Within this configuration, two paths have been created to balance exposure to magnetic flux with series connections between poles and across layers in two-layer units. Each path in this example is a grouping of eight turns each for a total of 64 series turns per layer. The paths from a single unit are connected in parallel as they have similar proximity to the ferrite. The two units of two-layer groups can then be connected in series, allowing for one parallel planar path by reducing the number of turns per layer by half. If effective, the transposition and parallel connections balance the phases and can handle three times as much current as the straightforward implementation.

IV. Simulation Studies With and Without Transposition

Voltage imbalances can cause large currents between the three phases due to the relatively low resistance and imbalances in self-inductance can lead to significant increases in cost due to varying capacitor size per phase. Induced voltage within the coil conductors can be calculated as:

$$\varepsilon = -N\frac{d\phi_B}{dt} \tag{3}$$

where ε is the induced voltage, N the number of turns and ϕ_B is the magnetic flux. Imbalances between phases and layers of conductors can be directly characterized by the difference in induced voltage, or flux linkage, as they are directly correlated with the change in magnetic flux. Systematic implementation of transposition can equalize the magnetic flux each conductor is exposed to, reducing imbalances accordingly.

A series of finite element simulations were created of the 100mm small-scale lab prototype 3-phase rotating-field coils to evaluate inductances and induced voltage with and without transposition at 85kHz. Induced voltage and inductance matrices were extracted directly to evaluate the effectiveness of conductor transposition. Both metrics are evaluated as the induced voltage magnitude is affected by input current while the calculated inductance matrix is not. The macro coil, a representative coil with the aggregate number of turns and layers, was used to minimize simulation mesh complexity. The simulations were created in 3D FEA as there is no symmetry with all three phases for the full rotating field excitation.

A model of the single-phase coil, shown in assembly view in Fig. 4 (a), was developed to compare inductance and induced voltage with and without the transposition. The variant without transposition assumed sequential layering of conductors without parallel paths and the variant with transposition with conductors arranged per paths one and two. The phase A coils were excited with 5.66Apk current at 85kHz, an amplitude calculated with mutual inductance results and (1) to reach an 11kW rated power. Induced voltage across layers in the coils with and without transposition had maximum differences of 0.4% and 31% respectively. Self-inductance across layers of the coils with and without transposition had maximum differences of 0.7% and 50% respectively. The results indicate that while there is a significant imbalance in the straightforward implementation, the transposition may effectively mitigate differences between layers. An example implementation of this transposition without fine turns within each group is shown in Fig. 4 (b) and was designed as a PCB with vias and six layers.

Three partial turn-by-turn models were created, two of which are depicted in Fig. 5, to evaluate non-linearity in loss at the skin depth. The first model was of three-phases for the

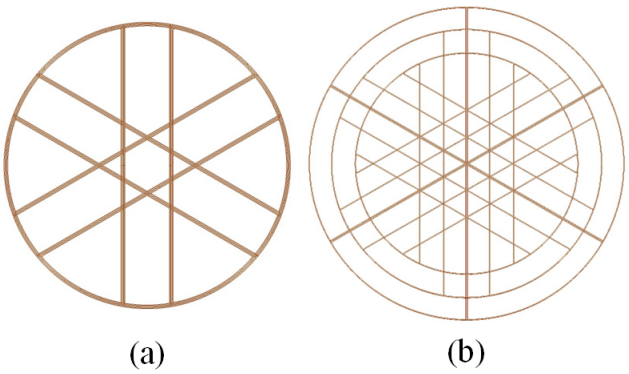

Fig. 5. Partial turn by turn models for three centermost turns (a) and the average turn, innermost turn, and outermost turn (b). The remainder of turns are omitted for clarity and reduced computational complexity.

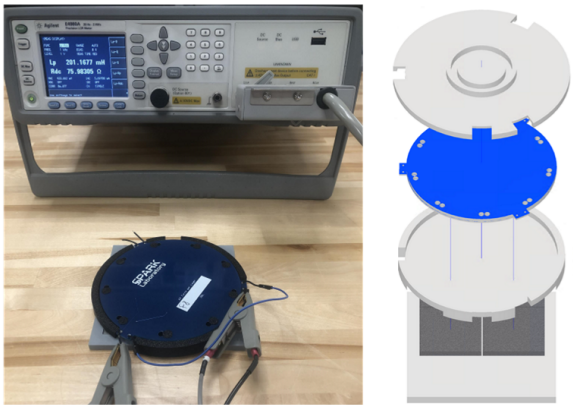

Fig. 7. Test configuration for validation of simulated coil inductances using an LCR meter and an assembly view of the non-conductive test fixture with a three-phase prototype and ferrite plates.

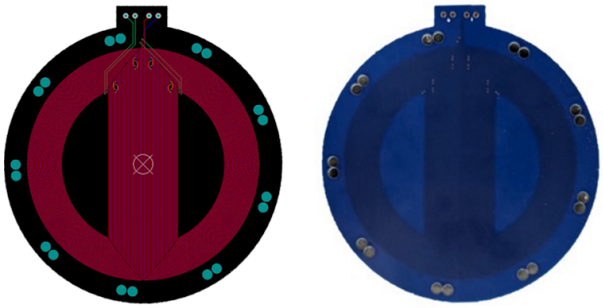

Fig. 6. Prototype coils employing parallel planar paths and the capability to connect in series/parallel between layers.

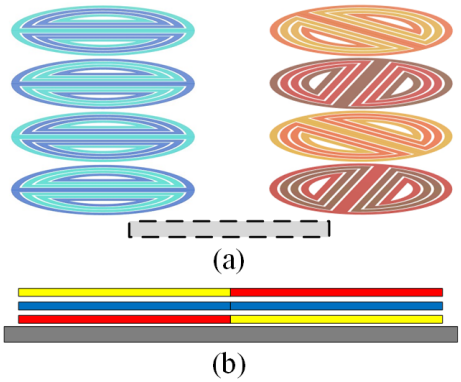

Fig. 8. Example transposition to balance parallel paths and phase proximity to the ferrite with paths per phase (a) and phase interleaving (b).

average turn, in this case a turn between turns 16 and 17 of 32, to establish the baseline results. The two other variants were for the three centermost turns, shown in Fig. 5 (a), and the average turn, innermost turn, and outermost turn, shown in Fig. 5 (b). In line with expectations, as the number of turns increased, the loss in each model increased linearly by the ratio of turns. Maximum accuracy would suggest simulation of a turn-by-turn model, but the lack of geometric symmetry requires a large mesh of multiple millions of tetrahedral elements. Results for the models with three centermost turns and three distributed turns required five times and eight times as many elements as the base case respectively.

A general method for the design of transposition can be developed using FEA to evaluate the variation of flux density across the coil. As the system does not physically rotate and the main magnetic material contributing to the flux is the ferrite core, magnetic flux is only dependent on active excitation. Magnetic flux density in the coils can be directly extracted from FEA across lines covering the vertical or horizontal component of the coil. Analysis of the resulting magnetic flux density vs distance can be used to decide upon the method of transposition depending on the proximity of layers or phases to the ferrite. Comparison between differences in induced voltage or flux linkage, both resulting from the integral of magnetic flux density across the coils, can confirm the effectiveness of transposition or be integrated into an optimization of coil parameters.

In principle, similar effects to transposition could be achieved by slightly varying the equivalent diameter of turns within a layer like that done in [13]. This method – which could also be combined with the proposed equivalent layer by layer transposition - may be implemented especially if the spacing between two adjacent traces is larger than the minimum acceptable dimension for the employed manufacturing techniques and equipment. Variation of diameter or conductor spacing conflict with either skin depth or manufacturing constraints respectively and require further study.

V. Experimental Measurements of Prototype Coils with Transposition

Two coils were designed as small-scale lab prototypes at a fixed 100mm outer diameter. One of the coils employed a single layer of coils to validate the simulated self and mutual inductance with the macro coil. The other coil employed the transposition from Fig. 3 to validate the capability to balance self and mutual inductances from the simulations and is shown in Fig. 6. Printed circuit board parameters for the example design had a trace width of 0.22mm, copper plate volume of

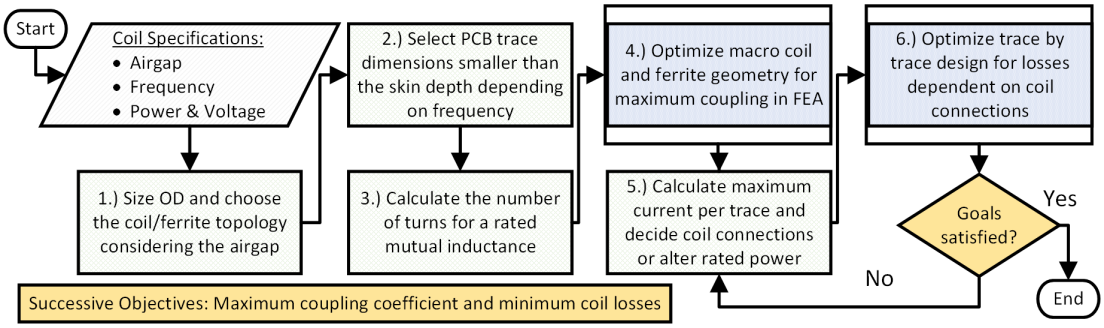

Fig. 9. Flowchart for a proposed two-step method for PCB WPT coil design, optimizing coupling coefficient using a macro coil model then designing wire by wire for loss mitigation. This method is possible as alteration of coupling coefficient and losses are largely independent from one another.

1oz., and a minimum space between conductors of 0.25mm. Four plates of 5mm thick, 50mm long PC95 ferrite squares were used for the ferrite core. A non-conductive test fixture was 3D printed, and is shown in Fig. 7 to mechanically offset the three PCB coils from one another and to align the ferrite.

The single layer prototype without transposition and was measured using an Agilent E4980A LCR meter in Lp-Rs mode with 85kHz excitation with the test-setup shown in Fig. 7. While measurement of self-inductance per coil simply required a connection to the positive and negative terminations of the coils, measurement of mutual inductance between phases required two steps. First, the measurements for series connections were made by connecting the negative of one coil to the positive of another and measuring across the terminals and anti-series connections by connecting the negatives of both coil and connecting across the positive terminals. Then, the following systems of equations is solved for mutual inductance, M, Ls = 2L + 2M and Las = 2L - 2M where L is self-inductance, Ls the series inductance, and Las the anti-series inductance. The resulting inductance matrix for three phases of the primary-side transmitter is tabulated in (4).

$$\begin{bmatrix} L_a & M_{ab} & M_{ac} \\ M_{ba} & L_b & M_{bc} \\ M_{ca} & M_{cb} & L_c \end{bmatrix} = \begin{bmatrix} 317 & -110 & -98 \\ -110 & 288 & -99 \\ -98 & -99 & 268 \end{bmatrix} \mu H \quad (4)$$

Macro coil simulations of the primary coils were created for both prototypes using the approximate value of coil span, outer diameter, and height of the copper conductors. The Z-axis position of conductors relative to the ferrite and the coil width had the largest impact on accuracy and were modified to match the prototypes. The resulting simulations had a $<5\%$ difference between measured and simulated self-inductances and a $<15\%$ difference in mutual inductances between phases in the prototype without transposition.

The simulated and experimental results from a single-phase of the prototype with transposition, shown in Fig. 6, indicate a less than 1% difference in self-inductance across paths. This suggests that the proposed transposition is effective, allowing for a mixture of series and parallel connections to increase efficiency for a rated power. Simulations for three-phases of the validated prototype resulted in equivalent self-inductance between paths for all three-phases with different inductances between phases due to the varying offset from the ferrite.

Interleaving phases between layers as shown in Fig. 8 may reduce phase to phase imbalance. Within this configuration, phases A and C are interwoven within one PCB and a single phase version of B is within another PCB in the stack as shown in Fig. 8 (a). The PCBs would then be combined as indicated in Fig. 8 (b) to balance relative proximity of all phases to the ferrite. This would allow for two parallel layers in phases A and C in both PCBs and four parallel layers in the phase B PCB and two coils connected in series per phase for more parallel planar paths. Future work will involve DC-DC operation of the primary and secondary sides with series-series compensation and GaN switches to evaluate system efficiency and effectiveness.

VI. Two-Step Optimization Method

A two-step design process, shown in Fig. 9, is proposed to maximize primary-secondary coupling through a macro coil model followed by the minimization of losses in the conductor to maximize coil efficiency at a rated power, airgap, and frequency. Two-step analysis is possible as the design parameters that affect coupling coefficient and losses in the coupler coil are largely decoupled. Optimization goals can be adjusted, for example, with reduction of cost, volume, or weight for transportation electrification.

The first stage maximizes coupling coefficient through systematic alteration of coil and ferrite geometry. Coupling coefficients can be directly extracted using the FEA in models with full primary and secondary modeled coils and a result from parametric studies. Studies were performed to evaluate which parameters, aside from the pre-defined conductor width, height, current, airgap, and OD, greatly affected coupling coefficient including the ratio of coil inner to outer radius, ferrite width, and ferrite height. A non-linearity was present for all three parameters from which values could be selected depending on the geometric limitations, increasing coupling coefficient by 18% relative to an initial design.

The second stage minimizes coil losses, requiring design down to the wire including the width and height of copper conductor, number of layers, the number and nature of series and parallel connections. Optimization of performance can be

considered against the respective variation in coil cost with a fixed outer diameter. Axial parallel connected layers and additional copper thickness can both decrease DC resistance but have different costs which increase non-linearly and are manufacturer dependent. Planned future work will include development of additional methods to simulate AC losses for the comparison of wire-to-wire design optimization.

VII. Conclusion

The proposed transposition can allow for increased rated power in three-phase rotating-field printed circuit boards with parallel connections by substantially mitigating inter-layer and inter-phase imbalances. The 3-phase rotating field topology was selected for its high specific power and designed with all possible techniques to improve current capability including innovative combinations of parallel split wires, transposition in multiple layers, and layer-to-layer connections. The limitations of current in printed circuit boards compared to Litz wire is discussed for high-frequency (85kHz) operation with potential methods of improvement using inter-layer connections and stacks of printed circuit boards.

A new method of transposition is proposed for single and three-phase bipolar rotating-field coils to allow for parallel layers to increase current carrying capability. Simulation results for self-inductance and interphase mutual inductance were validated with measurements of an experimental prototype. Additionally, simulation and experimental implementation of the proposed transposition matched as expected, enabling high rated power with parallel connections compared to single layer variants. A two-step design method is also proposed to optimize coupling effectiveness, maximizing the coupling coefficient through modification of coil and ferrite topology followed by an analytical optimization of conductor dimensions and layer-to-layer connections for the minimization of coil resistance.

Acknowledgment

This work was supported by the National Science Foundation (NSF) Graduate Research Fellowship under Grant No. 2239063. The support of the Leverhulme Trust under their visiting professorship scheme is also gratefully acknowledged. Any opinions, findings, and conclusions or recommendations expressed in this material are those of the authors and do not necessarily reflect the views of the sponsoring organizations. The authors are also thankful to ANSYS Inc. and University of Kentucky, the L. Stanley Pigman Chair in Power endowment.

References

[1] S. Li and C. C. Mi, "Wireless power transfer for electric vehicle applications," *IEEE Journal of Emerging and Selected Topics in Power Electronics*, vol. 3, no. 1, pp. 4–17, 2015.

[2] D. Patil, M. K. McDonough, J. M. Miller, B. Fahimi, and P. T. Balsara, "Wireless power transfer for vehicular applications: Overview and challenges," *IEEE Transactions on Transportation Electrification*, vol. 4, no. 1, pp. 3–37, 2018.

[3] Z. Ouyang and M. A. E. Andersen, "Overview of planar magnetic technology—fundamental properties," *IEEE Transactions on Power Electronics*, vol. 29, no. 9, pp. 4888–4900, 2014.

[4] A. Ramezani and M. Narimani, "An efficient PCB based magnetic coupler design for electric vehicle wireless charging," *IEEE Open Journal of Vehicular Technology*, vol. 2, pp. 389–402, 2021.

[5] Y. Liu, E. M. Dede, S. A. Khan, G. Liu, A. Kamineni, J. S. Lee, and M. Wang, "Thermal design and evaluation of a rectifier for electric vehicle wireless charging using hybrid pcbs and planar magnetics," *IEEE Transactions on Components, Packaging and Manufacturing Technology*, vol. 14, no. 5, pp. 766–775, 2024.

[6] F. Marcolini, G. D. Donato, F. Giulii Capponi, M. Incurvati, and F. Caricchi, "On winding manufacturing technologies for coreless axial-flux permanent-magnet machines," in *2023 IEEE Workshop on Electrical Machines Design, Control and Diagnosis (WEMDCD)*, 2023, pp. 1–7.

[7] Y. Chulaee, D. Lewis, A. Mohammadi, G. Heins, D. Patterson, and D. M. Ionel, "Circulating and eddy current losses in coreless axial flux PM machine stators with PCB windings," *IEEE Transactions on Industry Applications*, vol. 59, no. 4, pp. 4010–4020, 2023.

[8] G. François and B. Dehez, "Impact of slit configurations on eddy current and Joule losses in PCB windings of PM machines," in *2021 IEEE International Electric Machines & Drives Conference (IEMDC)*, 2021, pp. 1–7.

[9] J. Pries, V. P. Galigekere, O. C. Onar, G.-J. Su, R. Wiles, L. Seiber, J. Wilkins, S. Anwar, and S. Zou, "Coil power density optimization and trade-off study for a 100kW electric vehicle IPT wireless charging system," in *2018 IEEE Energy Conversion Congress and Exposition (ECCE)*, 2018, pp. 1196–1201.

[10] W. Chen, Y. Yan, Y. Hu, and Q. Lu, "Model and design of pcb parallel winding for planar transformer," *IEEE Transactions on Magnetics*, vol. 39, no. 5, pp. 3202–3204, 2003.

[11] P. Rehlaender, T. Grote, S. Tikhonov, H. Niejende, F. Schafmeister, J. Böcker, and P. Thiemann, "A PCB integrated winding using a Litz structure for a wireless charging coil," in *2019 21st European Conference on Power Electronics and Applications (EPE '19 ECCE Europe)*, 2019, pp. P.1–P.9.

[12] A. Narvaez, C. Carretero, I. Lope, and J. Acero, "Printed circuit board coils of multitrack litz structure for 3.3-kw inductive power transfer system," *IEEE Transactions on Transportation Electrification*, vol. 9, no. 3, pp. 3947–3957, 2023.

[13] R. Qin, J. Li, and D. Costinett, "A 6.6-kW high-frequency wireless power transfer system for electric vehicle charging using multilayer nonuniform self-resonant coil at MHz," *IEEE Transactions on Power Electronics*, vol. 37, no. 4, pp. 4842–4856, 2022.

[14] *Ansys® Electronics, Maxwell, version 24.1, 2024, ANSYS Inc.*

[15] D. D. Lewis, O. Onar, L. Gastineau, J. F. Eastham, and D. M. Ionel, "High-power polyphase PCB-Type inductive coupler for wireless electric vehicle charging," in *2024 IEEE Transportation Electrification Conference & Expo (ITEC)*, 2024.

[16] J. Pries, V. P. N. Galigekere, O. C. Onar, and G.-J. Su, "A 50-kW three-phase wireless power transfer system using bipolar windings and series resonant networks for rotating magnetic fields," *IEEE Transactions on Power Electronics*, vol. 35, no. 5, pp. 4500–4517, 2020.

[17] IPC (Organization), "IPC-2221 - Revision C - Standard Only Generic Standard on Printed Board Design," Dec. 2023. [Online]. Available: https://shop.ipc.org/ipc-2221/ipc-2221-standard-only/Revision-c/english

[18] "J2954_202208: Wireless Power Transfer for Light-Duty Plug-in/Electric Vehicles and Alignment Methodology - SAE International." [Online]. Available: https://www.sae.org/standards/content/j2954_202208/

[19] Z. Li, X. He, and Z. Shu, "Design of coils on printed circuit board for inductive power transfer system," *IET Power Electronics*, vol. 11, no. 15, pp. 2515–2522, 2018. [Online]. Available: https://ietresearch.onlinelibrary.wiley.com/doi/abs/10.1049/iet-pel.2018.5780